CAMBRIDGE
UNIVERSITY PRESS

Article

Luboržákite, Mn$_2$AsSbS$_5$, a new member of pavonite homologous series from Vorontsovskoe gold deposit, Northern Urals, Russia

Anatoly V. Kasatkin[1]* , Emil Makovicky[2], Jakub Plášil[3], Radek Škoda[4], Atali A. Agakhanov[1], Sergey Y. Stepanov[5] and Roman S. Palamarchuk[6]

[1]Fersman Mineralogical Museum of the Russian Academy of Sciences, Leninsky Prospekt 18-2, 119071 Moscow, Russia; [2]Department of Geoscience and Resource Management, University of Copenhagen, Østervoldgade 10, DK-1350, Copenhagen K, Denmark; [3]Institute of Physics ASCR, v.v.i., Na Slovance 1999/2, 18221 Praha 8, Czech Republic; [4]Department of Geological Sciences, Faculty of Science, Masaryk University, Kotlářská 2, 611 37, Brno, Czech Republic; [5]Department of Minerals Deposits Geology, St. Petersburg State University, University Embankment 7/9, 199034 St Petersburg, Russia; and [6]South Urals Federal Research Center of Mineralogy and Geoecology, Ural Branch of the Russian Academy of Sciences, territory of the Ilmeny State Reserve, Miass, Chelyabinsk District, 456317, Russia

Abstract

Luboržákite, ideally Mn$_2$AsSbS$_5$, is a new mineral from the Vorontsovskoe gold deposit, Northern Urals, Russia. It forms long-prismatic crystals up to 70×20 μm and anhedral grains of the same size embedded in the matrix of Mn-bearing dolomite and Mn-bearing calcite. Associated minerals include pyrite, orpiment, realgar, stibnite, aktashite, alabandite, boscardinite, chabournéite, coloradoite, clerite, écrinsite, gold, routhierite, sphalerite and twinnite. Luboržákite is black, opaque with metallic lustre and has a black streak. It is brittle and has an uneven fracture. No cleavage and parting have been observed. Mohs hardness is 4–4½. $D_{calc} = 4.181$ g cm^{-3}. In reflected light, luboržákite is tin-white, weakly anisotropic with rotation tints varying from dark grey to grey. The chemical composition of luboržákite is (wt.%; electron microprobe, WDS mode): Mn 21.23, Cu 0.29, Ag 0.56, Pb 1.90, As 15.25, Sb 27.03, S 33.23, total 99.49. The empirical formula based on the sum of all atoms = 9 apfu is Mn$_{1.86}$Pb$_{0.04}$Ag$_{0.03}$Cu$_{0.02}$As$_{0.98}$Sb$_{1.07}$S$_{5.00}$. The new mineral is monoclinic, space group $C2/m$ with $a = 12.5077(6)$, $b = 3.8034(2)$, $c = 16.0517(8)$ Å, $\beta = 94.190(4)°$, $V = 761.57(6)$ Å^3 and $Z = 4$. The crystal structure of luboržákite was solved from the single-crystal X-ray diffraction data to $R = 0.0383$ for 712 observed reflections with $I > 3\sigma(I)$. Luboržákite is a new member of the heterochemical isostructural series of 'unit-cell twinned' structures, named the pavonite series. The new mineral honours Lubor Žák, a prominent Czech crystallographer and the professor of the Charles University in Prague, Czech Republic.

Keywords: luboržákite, Mn$_2$AsSbS$_5$, new mineral, chemical composition, crystal structure, pavonite homologous series, Vorontsovskoe deposit, Northern Urals

(Received 20 May 2020; accepted 4 June 2020; Accepted Manuscript published online: 10 June 2020; Associate Editor: Juraj Majzlan)

Introduction

Over the last eight years, our team has systematically investigated the mineralogy of the actively exploited Vorontsovskoe gold deposit in the Northern Urals. This deposit is unique in Russia concerning its Mn–Tl–Hg–As–Sb mineralisation. Moreover, our studies have revealed an outstanding diversity of rare sulfosalts discovered there, four of which have already been described as entirely new to science: vorontsovite, ferrovorontsovite (Kasatkin *et al.*, 2018*a*), tsygankoite (Kasatkin *et al.*, 2018*b*) and gladkovskyite (Kasatkin *et al.*, 2019). Herein we describe luboržákite, the fifth new sulfosalt from this deposit and a new member of the pavonite homologous series.

Luboržákite (pronounced: lu bor zha kait; cyrilic – люборжакит) honours Prof. RNDr. Lubor Žák, CSc. (born in Prague, July 29, 1925 and died in Prague, August 6, 2008). For all of his professional life, Professor Žák was connected with

the Faculty of Science of Charles University in Prague. He was an excellent crystallographer and mineralogist; one of the leading persons in the former Czechoslovakia of the second half of the 20th Century, who maintained a high level of mineralogical crystallography. Among other topics, he focused his research on the mineralogy and structures of Bi-sulfosalts. In particular, he described such minerals as krupkaite (Žák *et al.*, 1974), paděraite (Mumme and Žák, 1985) and a member of pavonite homologous series makovickyite (Žák *et al.*, 1994). His other professional passion comprised geology and mineralogy of manganese deposits in former Czechoslovakia, like Chvaletice (e.g. Žák, 1972; Žák and Povondra, 1981). Taking into consideration the above, we found it particularly appropriate to name a new member of the pavonite homologous series, with Mn as a species-defining element, after Prof. Žák.

The new mineral and its name have been approved by the Commission on New Minerals, Nomenclature and Classification of the International Mineralogical Association (IMA2019-125, Kasatkin *et al.*, 2020). The holotype specimen is deposited in the collections of the Fersman Mineralogical Museum of the Russian Academy of Sciences, Moscow, Russia, with the registration number 5498/1.
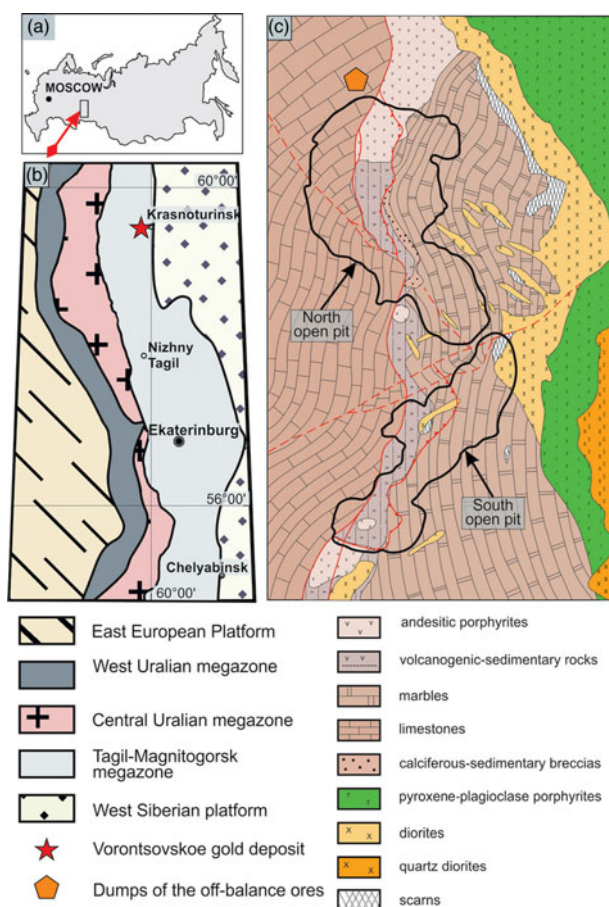
Fig. 1. Geographical position and geological map of the Vorontsovskoe gold deposit. Modified after Minina (1994) and Vikentyev et al. (2016).

Fig. 2. Collecting specimens at dumps of the off-balance ores where luboržákite was found. August 2017. Photo: V.A. Saltanov.

Occurrence: geological settings and ore-mineral association

The Vorontsovskoe gold deposit was discovered in 1985 and is operated currently by the Russian mining company Polymetal International plc for high-grade gold-bearing ore. In 2019 the company extracted 1050 million tons of ore and produced 107.000 tr.oz (∼3.3 tons) of refined gold. The ore reserves at 01/01/2020 were estimated as 1.5 million tr.oz of gold with an average content of 2.0 g/t (data taken from the official website https://www.polymetalinternational.com/ru/assets/where-we-operate/voro/).

Geographically, the Vorontsovskoe gold deposit is located in Northern Urals, ∼13 km to the south of the city of Krasnotur'insk, Sverdlovskaya Oblast' and ∼370 km to the north of Ekaterinburg (Fig. 1a,b).

Geologically, it is situated inside the Auerbakh ore cluster, at the western exocontact of the Early Devonian Auerbakh gabbro–diorite–granodiorite massif, which intrudes sedimentary and volcano-sedimentary rocks. At the regional scale, the Auerbakh massif is located in the eastern part of the Tagil–Magnitogorsk megazone between Central Uralian megazone and West Siberian platform (Fig. 1b). The formation of magmatites of Auerbakh intrusion is a result of the development of the Tagil island arc. The Vorontsovskoe deposit comprises a tectonic monocline, which is composed of volcanogenic–sedimentary rocks: tuffs, siltstones and tuffaceous sedimentary rocks (Fig. 1c). This monocline is limited by a substantial tectonic fault where it contacts carbonate rocks, such as limestone and marble. Both the volcanogenic–sedimentary rocks and the limestones underwent metasomatic processes and were partially replaced by different metasomatites (skarns, argillisites and jasperoids) with ore concentrations of gold. The main volume of gold, however, is related genetically to fluid-explosive breccias cemented typically by pyrite, realgar, orpiment and stibnite. Both the limestones and volcanogenic–sedimentary rocks are brecciated. These breccias bear a unique Tl–Hg–Pb–Mn mineralisation with many rare sulfosalts distributed widely in ore cement (Fershtater, 2013; Vikentyev et al., 2016; Murzin et al., 2017; Stepanov et al., 2017; Kasatkin et al., 2019). In general, the spatial combination of different volcanogenic–sedimentary and carbonate rocks replaced by various metasomatites, together with the development of fluid-explosive breccias, resulted in the formation of a unique mineral paragenesis including the new mineral described below.

Specimens containing luboržákite were collected in August 2017 at the dumps of the off-balance ores of the deposit (59° 39'28"N, 60°12'41"E) (Figs 1c, 2). The new mineral was found in carbonate breccias composed mainly of Mn-bearing calcite and Mn-bearing dolomite and cemented by fine-grained pyrite, realgar and stibnite (Fig. 3). Associated minerals of sulfide–sulfosalt assemblage also include Mn-bearing aktashite, alabandite, boscardinite, chabournéite, coloradoite, clerite, écrinsite, gold, orpiment, routhierite, Mn-rich sphalerite, twinnite and several potentially new Mn-bearing phases. Other minerals directly associating with luboržákite are baryte, chernovite-(Y), diopside, fluorapatite, hyalophane, muscovite and prehnite.

The mineral association described above is connected with a rich pyrite–realgar–stibnite type of ore. Another specific feature is an enrichment of the ore system in Mn sourced from sedimentary and volcanogenic–sedimentary rocks. Apart from its high concentrations in carbonates (Mn-bearing calcite and dolomite) and wide distribution of alabandite and Mn-rich sphalerite, this association is the only one at the deposit that includes two sulfosalts (luboržákite and clerite) with Mn as a species-defining element, without essential Tl.

The main features of this ore-mineral association allow us to suggest a particular mineral sequence. The formation of the cement in the ore breccias in earlier, high-temperature stages was accompanied by the crystallisation of primary sulfides such as pyrite, stibnite, alabandite and sphalerite. The gradual decrease of temperature led to the crystallisation of realgar and orpiment

Fig. 3. Carbonate breccias with pyrite, realgar and stibnite, where luboržákite was discovered, *in situ*, August 2017. FOV: 13 cm x 9 cm. Photo: S.Y. Stepanov.

followed by the formation of the main volume of the rare Mn-, Tl-, Hg- and Pb-bearing sulfosalts such as luboržákite, aktashite, boscardinite, chabournéite, clerite, écrinsite, routhierite and twinnite. The uniform distribution of sulfarsenites and sulfantimonites results from the saturation of the ore-forming environment both by As and Sb. It is not surprising then that in the chemical composition of the majority of studied sulfosalts, significant contents of both

As and Sb are found. The same applies to Mn: the general enrichment of the system by this element reflects on the chemistry of associated sulfosalts. While luboržákite and clerite contain Mn as a species-defining cation, all the others (except routhierite and twinnite) have Mn as a small admixture. The list of all above mentioned rare sulfosalts identified by us in association with luboržákite, their chemical data and refined unit–cell parameters are given in Table 1.

General appearance and physical properties

Luboržákite occurs as long-prismatic crystals up to 70 μm × 20 μm and anhedral grains of the same size embedded in the matrix of Mn-bearing dolomite and Mn-bearing calcite (Fig. 4). Sometimes it forms partial pseudomorphs after earlier alabandite. A similar relationship was observed by us in different mineral associations: between alabandite and tsygankoite (Kasatkin *et al.*, 2018*a*) and alabandite and gladkovskyite (Kasatkin *et al.*, 2019). Luboržákite is black and opaque. It has a metallic lustre and a black streak. The mineral is brittle and has an uneven fracture. No cleavage and parting are observed. Luboržákite does not exhibit any fluorescence under ultraviolet radiation. The Vickers hardness (VHN, 30 g load) is 242 kg/mm^2 (range 236–248 kg/mm^2, $n = 3$) corresponding to a Mohs hardness of 4–4½. The density of luboržákite could not be measured because of the absence of suitable

Table 1. Chemical composition and unit-cell parameters of rare sulfosalts identified in the association with luboržákite (our data).

	Aktashite	Boscardinite	Chabournéite	Clerite	Écrinsite	Routhierite	Twinnite
Chemical composition*							
Wt.%							
Mn	1.02	0.14	0.03	13.77	0.30	–	–
Cu	26.19	0.02	0.01	–	–	5.98	–
Zn	3.01	–	–	–	–	1.02	–
Ag	–	1.51	0.07	–	1.21	0.63	–
Hg	25.75	–	–	–	–	36.52	–
Tl	–	12.60	18.85	–	8.41	20.95	2.95
Pb	–	21.32	10.31	–	30.71	0.09	34.02
As	18.30	12.19	16.61	4.64	15.74	14.52	10.40
Sb	0.94	29.16	29.83	51.91	19.92	1.30	27.77
S	25.38	24.52	25.46	30.87	24.77	18.60	24.41
Total	100.59	101.46	101.17	101.19	101.06	99.61	99.55
Atoms per formula unit							
Mn	0.28	0.12	0.02	1.03	0.26	–	–
Cu	6.25	0.01	0.01	–	–	0.95	–
Zn	0.70	–	–	–	–	0.16	–
Ag	–	0.66	0.03	–	0.53	0.06	–
Hg	1.95	–	–	–	–	1.84	–
Tl	–	2.93	3.94	–	1.95	1.04	0.08
Pb	–	4.88	2.13	–	7.01	0.01	0.88
As	3.70	7.72	9.47	0.25	9.94	1.96	0.74
Sb	0.12	11.37	10.47	1.75	7.74	0.11	1.22
S	12.00	36.30	33.93	3.97	36.56	5.87	4.08
Total	25	64	60	7	64	12	7
Unit–cell parameters**							
Crystal system	Trigonal	Triclinic	Triclinic	Orthorhombic	Triclinic	Tetragonal	Monoclinic
a (Å)	13.639(4)	8.080(1)	16.21(2)	11.4021(12)	8.034(8)	9.967(5)	7.9846(13)
b (Å)		8.730(2)	42.44(6)	14.3790(15)	8.533(4)		19.472(2)
c (Å)	9.303(7)	22.474(4)	8.60(1)	3.7908(4)	22.320(9)	11.382(10)	8.6127(17)
α (°)		90.78(1)	83.9(2)		90.58(5)		
β (°)		97.08(1)	89.9(1)		96.96(8)		90.817(17)
γ (°)		90.93(1)	83.6(2)		90.63(7)		
V (Å^3)	1499(1)	1572.8(3)	5844(8)	621.50(11)	1519(2)	1131(1)	1338.9(4)

* Electron microprobe, WDS mode; each analysis is the average of 5 spot analyses
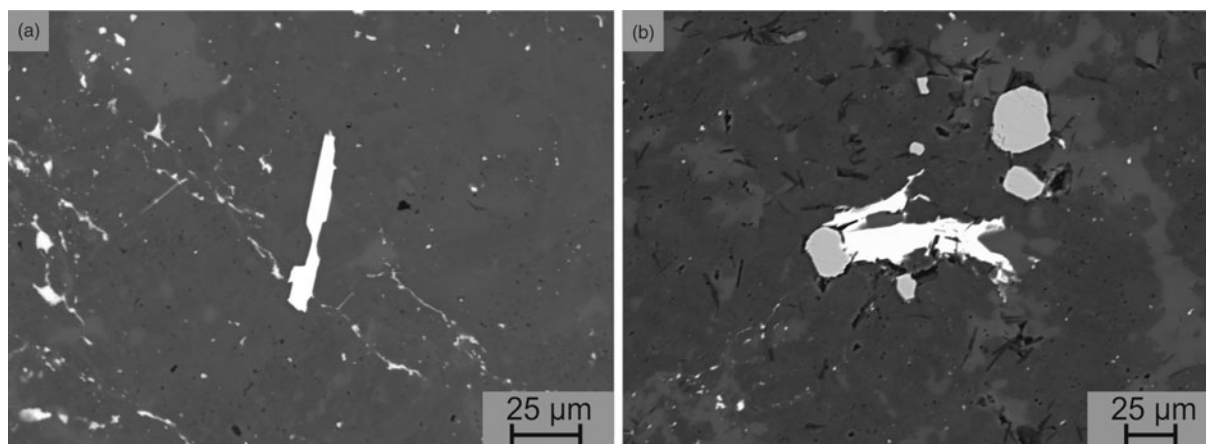** Single-crystal X-ray data
– = below detection limit

Fig. 4. Long-prismatic crystals of luboržákite (white) in Mn-bearing dolomite (dark grey) and Mn-bearing calcite (medium grey) matrix with pyrite (light grey rounded grains on photo 4b). Polished section. Back-scattered electron image.

Table 2. Reflectance data of luboržákite in %.

λ (nm)	R_{min}	R_{max}	λ (nm)	R_{min}	R_{max}
400	24.3	26.9	560	22.3	24.6
420	23.9	26.4	580	22.1	24.4
440	23.7	26.2	**589**	**22.1**	**24.3**
460	23.7	26.0	600	22.0	24.2
470	**23.6**	**25.3**	620	22.0	24.1
480	22.9	25.2	640	21.9	24.1
500	22.9	25.2	**650**	**21.8**	**23.8**
520	22.7	24.8	660	21.4	23.5
540	22.4	24.8	680	21.3	23.4
546	**22.4**	**24.7**	700	21.0	23.1

The values recommended by the Commission on Ore Microscopy (COM) are marked in bold.

Table 3. Average chemical composition of luboržákite (wt.%).

Constituent	Wt.%	Range	S.D.	Probe standard
Mn	21.23	20.62–21.81	0.43	Mn
Cu	0.29	0.17–0.38	0.08	Cu
Ag	0.56	0.39–0.93	0.19	Ag
Pb	1.90	0.19–3.89	1.49	PbSe
As	15.25	14.64–15.72	0.36	Pararammelsbergite
Sb	27.03	25.51–28.74	1.49	Sb
S	33.23	32.51–33.74	0.48	Chalcopyrite
Total	99.49			

S.D. = standard deviation

heavy liquids and paucity of available pure material. The density calculated based on the empirical formula ($Z = 4$) and the unit-cell volume determined from the single-crystal X-ray diffraction data is 4.181 g/cm^3.

In reflected light, luboržákite is tin-white and non-pleochroic. The bireflectance is distinct, $\Delta R = 2.2\%$ (589 nm). Under crossed polars the new mineral is weakly anisotropic with rotation tints varying from dark grey to grey. Internal reflections are not observed. Quantitative reflectance measurements were performed in the air relative to a WTiC standard using a Universal Microspectrophotometer UMSP 50 (Opton-Zeiss, Germany). Reflectance values are given in Table 2.

Chemical composition

Five electron-microprobe analyses were carried out with a Cameca SX-100 electron microprobe (WDS mode with an accelerating voltage of 25 kV, a beam current on the specimen of 10 nA and a beam diameter of 2 µm). Peak counting times were 20 s for all elements; counting time for each background was one-half of the peak time. The raw intensities were converted into concentrations using X-PHI (Merlet, 1994) matrix-correction software.

Analytical data and standards used are given in Table 3. Contents of other elements with atomic numbers higher than that of carbon are below detection limits. The empirical formula (based on the sum of all atoms = 9 atoms per formula unit) is: $Mn_{1.86}Pb_{0.04}Ag_{0.03}Cu_{0.02}As_{0.98}Sb_{1.07}S_{5.00}$. The ideal chemical formula is Mn_2AsSbS_5, which requires Mn 23.54, As 16.05, Sb 26.07, S 34.34, total 100 wt.%.

X-ray diffraction data

A blocky fragment of luboržákite, 18 µm × 13 µm × 1 µm in size, extracted from the polished section analysed using electron microprobe, was mounted on glass fibre and examined with a Rigaku SuperNova single-crystal diffractometer equipped with an Atlas S2 CCD detector and a microfocus MoKα source. Data reduction was performed using CrysAlisPro Version 1.171.39.46 (Rigaku, 2019). The data were corrected for Lorentz factor, polarisation effect and absorption (multi-scan, ABSPACK scaling algorithm; Rigaku, 2019).

The monoclinic unit-cell parameters determined from single-crystal data are as follows: $a = 12.5077(6)$ Å, $b = 3.8034(2)$ Å, $c = 16.0517(8)$ Å, $β = 94.190(4)°$, $V = 761.57(6)$ Å^3 and $Z = 4$ with the space group $C2/m$.

Due to a poorly diffracting crystal of extremely small size, only the calculated powder pattern is given in Table 4. Theoretical data were obtained using the program PowderCell (Kraus and Nolze, 1996).

The crystal structure of luboržákite was solved from single-crystal X-ray data using the charge-flipping algorithm of the program SHELXT (Sheldrick, 2015) and refined by the software Jana2006 (Petříček et al., 2014) to R = 0.0383 for 712 independent reflections with $I > 3σ(I)$. The crystal data and the experimental details are listed in Table 5, atom coordinates, atomic displacement parameters and site occupancies in Table 6 and selected interatomic distances in Table 7. The crystallographic information

Table 4. Calculated powder X-ray data (d in Å) for luboržákite (only diffractions with I_{rel}.>5% are listed).

I_{calc}.	d_{calc}.	h k l
7	16.009	0 0 1
11	8.004	0 0 2
6	6.237	2 0 0
16	5.961	$\bar{2}$ 0 1
19	5.104	$\bar{2}$ 0 2
12	4.754	2 0 2
7	4.210	$\bar{2}$ 0 3
11	4.002	0 0 4
24	3.916	2 0 3
50	**3.486**	**$\bar{2}$ 0 4**
10	3.339	$\bar{1}$ 1 2
50	**3.286**	**1 1 2**
36	**3.262**	**2 0 4**
11	3.202	0 0 5
5	3.119	4 0 0
5	3.104	$\bar{4}$ 0 1
19	3.036	$\bar{1}$ 1 3
6	3.020	4 0 1
17	2.937	$\bar{2}$ 0 5
39	2.806	3 1 0
57	2.788	$\bar{3}$ 1 1
29	2.767	2 0 5
27	2.741	3 1 1
100	**2.690**	**$\bar{3}$ 1 2**
30	2.609	3 1 2
12	2.521	$\bar{2}$ 0 6
9	2.435	3 1 3
8	2.391	2 0 6
6	2.377	4 0 4
6	2.200	$\bar{2}$ 0 7
19	2.174	$\bar{1}$ 1 6
24	2.130	1 1 6
9	2.001	0 0 8
10	1.987	$\bar{6}$ 0 3
9	1.977	6 0 2
7	1.955	$\bar{1}$ 1 7
10	1.918	1 1 7
37	**1.904**	**5 1 3**
9	1.903	$\bar{6}$ 0 4
36	**1.902**	**0 2 0**
13	1.898	5 1 4
5	1.891	6 0 3
6	1.866	2 0 8
10	1.817	$\bar{3}$ 1 7
22	1.799	$\bar{5}$ 1 5
14	1.769	$\bar{1}$ 1 8
9	1.670	$\bar{2}$ 2 4
7	1.643	2 2 4
5	1.616	$\bar{7}$ 1 1
6	1.567	2 2 5
7	1.541	8 0 1

The strongest lines are given in bold

file has been deposited with the Principal Editor of *Mineralogical Magazine* and is available as Supplementary material (see below).

Crystal structure

The structure of luboržákite contains ten atomic sites; one site occupied purely by Sb, one site occupied purely by Mn, five S sites, and three mixed-occupied sites: two As/Mn sites and one Mn/Sb site.

The structural formula of the mineral can be written as $[Mn_{0.5}SbS_2]^{thin\_layer} \cdot [(Mn,Sb)_{0.5}(AsMn)_{\Sigma 2}S_3]^{thick\_layer}$, individualising

Table 5. Summary of data collection conditions and refinement parameters for luboržákite.

Crystal data	
Chemical formula	$Mn_{1.921}Sb_{1.106}S_5As_{0.974}$
Crystal size (mm)	0.018 × 0.013 × 0.011
Crystal system	monoclinic
Space group	C2/m
Temperature (K)	289
Unit-cell parameters:	
a, b, c (Å)	12.5077(6), 3.8034(2), 16.0517(8)
β (°)	94.190(4)
Unit-cell volume (Å³)	761.57(7)
Z	4
Calculated density (g/cm³) (from the structural formula)	4.131
Data collection	
Diffractometer	Rigaku SuperNova with Atlas S2 CCD
Radiation, wavelength (Å)	MoKα, 0.71073 (50 kV, 30 mA)
θ range for data collection (°)	2.54 – 28.46
Limiting Miller indices	$-16 \leq h \leq 14$, $-5 \leq k \leq 4$, $-21 \leq l \leq 21$
Axis, frame width (°), time per frame (s)	ω, 1.0, 500
Total reflections collected	5255
Unique reflections	982
Unique observed reflections, criterion	712, ($I > 3\sigma(I)$)
Absorption coefficient (mm⁻¹), type	12.49; multi-scan
T_{min}/T_{max}	0.911/1
Data completeness to θ_{max} (%), R_{int}	89.00, 0.041
Refinement	
Structure refinement	Full-matrix least-squares on F^2
No. of param., restraints, constraints	60, 0, 16
R, wR (obs)	0.0382, 0.0659
R, wR (all)	0.0682, 0.0717
Gof obs/all	1.64, 1.50
Weighting scheme, weights	σ, $w = 1/(\sigma^2(I) + 0.0004I^2)$
$\Delta\rho_{max}$, $\Delta\rho_{min}$ ($e^-/Å^3$)	3.78, −2.05

two layers in its structure, or, alternatively, as $Mn_{0.5}(Mn,Sb)_{0.5}(AsMn)_{\Sigma 2}SbS_5$.

Luboržákite is a new member of the heterochemical isostructural series of 'unit-cell twinned' structures, named the 'pavonite series' after the first analysed member, pavonite $AgBi_3S_5$ (Makovicky *et al.*, 1977). These structures resemble the unit-cell-twinned lillianite, in which slabs of PbS-like arrangement are cut along $(311)_{PbS}$ and twinned using these planes *via* bi-capped trigonal coordination prisms (of mostly Pb). In the pavonite series, one orientation of these slabs is always only one octahedron-wide, whereas the other, intervening slab orientation, can be several cation-coordination octahedra wide (up to 8 octahedra). The bi-capped trigonal coordination prisms on twin planes become distorted and are usually occupied by the lone electron pair of Bi (or Sb) situated in one of the prism's caps. Newer summaries concerning this series can be found in e.g. Makovicky (2006, 2019), and literature dealing with new members of the series.

In luboržákite, the octahedron of the thinner layer (Figs 5 and 7) is occupied by Mn3, whereas the caps of the 'empty', only moderately distorted trigonal coordination prisms have the cap which is oriented into this layer filled by a coordination prism of Sb1. Typical short Sb–S distances of 2.51 Å and 2.61 Å indicate a pure antimony site. The Mn octahedron is slightly foreshortened, with 2.62 Å in the octahedral waist and only 2.53 Å to the 'horizontally' lying vertices (Fig. 5). The thicker slab is five octahedra thick (measured in the $(100)_{PbS}$ plane, which runs across the slab, diagonally to the $(311)_{PbS}$ surface of the slab,

Table 6. Sites, site occupancy factors, atom factional coordinates, and equivalent isotropic displacement parameters (in Å^2) for luboržákite.

Atom	x/a	y/b	z/c	U_{eq}
Sb1	0.70359(5)	1	0.38410(4)	0.0260(2)
*As2/As2'	0.45606(11)	½	0.20441(8)	0.0329(5)
*Mn2/Mn2'	½	0	0	0.0384(7)
*As3/As3'	0.23266(10)	0	0.11593(9)	0.0383(5)
Mn3	½	½	½	0.0202(6)
S1	0.64205(17)	1	0.52920(13)	0.0159(6)
S2	0.56273(17)	½	0.35382(13)	0.0200(7)
S3	0.34236(19)	0	0.24368(15)	0.0251(8)
S4	0.3725(2)	½	0.05194(16)	0.0344(9)
S5	0.1105(2)	−½	0.15108(19)	0.0427(10)

*Occupancies: As2/As2' = 0.441(16) As/0.559(16) Mn; Mn2/Mn2' = 0.789(8) Mn/0.211(8) Sb; As3/As3' = 0.532(18) As/0.468(18) Mn

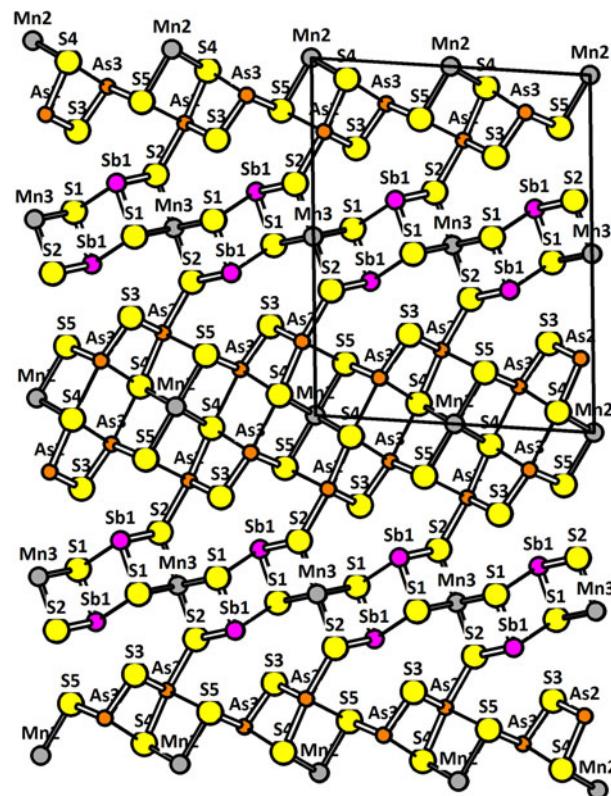**Table 7.** Selected interatomic distances (in Å) in luboržákite.

Sb1–S1	2.5061(19)	Mn2/Mn2'–S4^i	2.6548(19)
Sb1–S1^{iii}	2.9817(18)	Mn2/Mn2'–S4	2.6548(19)
Sb1–S1^{iv}	2.9817(18)	Mn2/Mn2'–S4^{xiii}	2.6548(19)
Sb1–S2	2.6140(17)	Mn2/Mn2'–S4^{ix}	2.6548(19)
Sb1–S2^{ii}	2.6140(17)	Mn2/Mn2'–S5^v	2.702(3)
		Mn2/Mn2'–S5^{xii}	2.702(3)
As2/As2'–S2	2.657(2)		
As2/As2'–S3	2.4835(18)		
As2/As2'–S3^{ii}	2.4835(18)	Mn3–S1^i	2.6209(17)
As2/As2'–S4	2.591(3)	Mn3–S1	2.6209(17)
As2/As2'–S5^v	2.884(2)	Mn3–S1^{viii}	2.6209(17)
As2/As2'–S5^{vi}	2.884(2)	Mn3–S1^{vii}	2.6209(17)
		Mn3–S2	2.5281(18)
As3/As3'–S3	2.383(2)	Mn3–S2^{vii}	2.5281(18)
As3/As3'–S4^i	2.827(2)		
As3/As3'–S4	2.827(2)		
As3/As3'–S4^{xi}	2.910(3)		
As3/As3'–S5	2.529(2)		
As3/As3'–S5^{ii}	2.529(2)		

Symmetry codes: (i) x, $y − 1$, z; (ii) x, $y + 1$, z; (iii) $−x + 3/2$, $y − ½$, $−z + 1$; (iv) $−x + 3/2$, $y + ½$, $−z + 1$; (v) $x + ½$, $y + ½$, z; (vi) $x + ½$, $y + 3/2$, z; (vii) $−x + 1$, y, $−z + 1$; (viii) $−x + 1$, $y − 1$, $−z + 1$; (ix) $−x + 1$, y, $−z$; (x) $x + ½$, $y − ½$, z; (xi) $−x + ½$, $y − ½$, $−z$; (xii) $x + ½$, $y + ½$, $−z$; (xiii) $−x + 1$, $y − 1$, $−z$.

Fig. 5. Projection of the crystal structure of luboržákite down **b**. Only strong short bonds are indicated.

Fig. 6). From the margin, it contains the As2–As3–Mn2–As3–As2 sites; all of the As sites contain a portion of Mn and possibly small amounts of Sb; the situation was refined as the As–Mn mixtures, with the same coordinates for both elements. The mixing is very clearly reflected by interatomic distances (Table 7) and displacement parameters of atoms.

The substitutional disorder (modelled as 0.21 Sb replacing 0.79 Mn) is reflected in high displacement values, not only of Mn2 itself (Sb does not occur in regular octahedral coordination with S, but as 3 + 3 sets of very different bonds), but also as a positional disorder in the S4 and especially S5 sites. The nearly 50:50 replacement of As by Mn in the marginal As3 sites does not disturb S2 appreciably but results in a high displacement of 'As3' itself and contributes to the positional disorder of two S4 atoms, shared with the above mentioned, substituted Mn2 site. Finally, As2, which is also approximately 50/50 occupied by As and Mn, with a slight prevalence of Mn over As, has a similar relationship to S2 and S3 as did As3, not leading to augmented displacement parameters. The positional disorder affects the other S atoms in its sphere, S4 and S5, which are shared with an Mn2 octahedron.

All diagonal interspaces in the thicker slab are moderately augmented lone electron pair micelles between the (100)$_{PbS}$ planes. They are placed *en echelon* and closed at both ends by strong short bonds As2 (and As3)–S (Fig. 7).

Discussion

The existence of the little distorted PbS-type slab composed of As polyhedra in luboržákite is a result of Mn substitution in all As positions. Otherwise, As – an element with extreme lone electron pair activity – would build arrays based on the SnS-like configurations. We can compare the present situation with the modifications/distortions in the PbS-like portions of the crystal structure of chabournéite (Biagioni *et al.*, 2015), which stem from a slightly 'uncomfortable' accommodation of lone-electron pairs of As and Sb.

The foreshortened Mn3 octahedron in the thinner layer and elongated Mn2 octahedron is suggestive of the Jahn–Teller effect, which dictates such deviations from the ideal octahedral shape, if manganese is trivalent and not divalent. Although cautioning that the shape might also have been influenced by the coordination requirements of the surrounding cations, and asking whether this mechanism works in sulfides, we think it worthy of mention here.

Luboržákite is a new member of the pavonite homologous series with $N = 5$ (^{5}P), like the ^{5}P pavonite, AgBi$_3$S$_5$, itself. It is interesting to compare the lattice parameters of these two compounds with the same space group of symmetry: $a = 13.305$ Å, $b = 4.042$ Å, $c = 16.417$ Å, $β = 94.02°$ for pavonite (Makovicky *et al.*, 1977), and $a = 12.5077$ Å, $b = 3.8034$ Å, $c = 16.0517$ Å, $β = 94.19°$ for luboržákite. The a and b values are influenced by the 'exchange' of Pb for Mn, whereas the c values reflect the strong lone-electron pair activity of As.
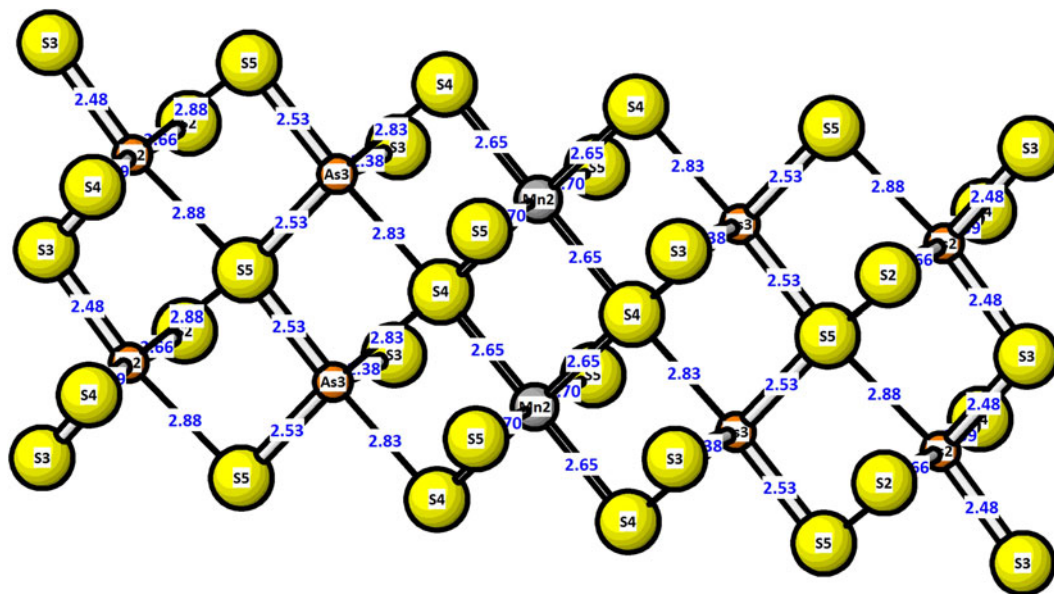
Fig. 6. Atom labelling and bond-distances for octahedral sites within a thick layer of the crystal structure of luboržákite.
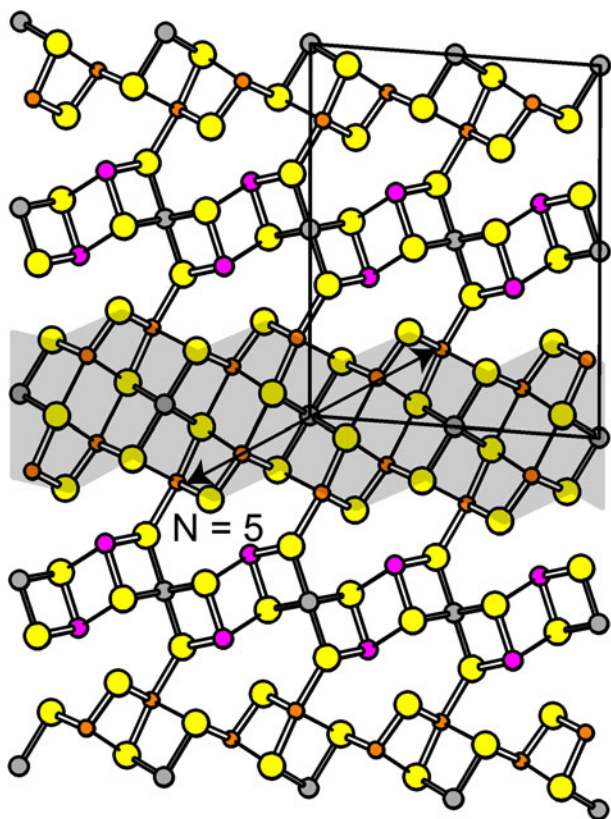

Fig. 7. The crystal structure of luboržákite projected down the **b** axis (∼3.8 Å) with alternating thin and thick (shaded) layers. Thick slabs contain five octahedral sites, defining it as a ^{5}P homologue of the pavonite homologous series. Atoms are colour-coded identically to Fig. 5.

Luboržákite is only the second member of the series having Mn as a species-defining cation after gražianite $MnBi_2S_4$ ($N = 3$) (Ciobanu *et al.*, 2014). The synthetic monoclinic modification of $MnSb_2S_4$ (Pfitzner and Kurowski, 2000) is the homologue

$N = 2$ (^{2}P), with Mn in both layer types which, accidentally, are almost identical in ^{2}P but still preserve some differences. For comparison, $a = 12.747$ Å, $b = 3.799$ Å, $c = 15.106$ Å and $\beta = 113.91°$ for this compound. Its natural dimorph, clerite, $MnSb_2S_4$ (Murzin *et al.*, 1996), that occurs in close association with luboržákite, has orthorhombic symmetry instead and belongs to the berthierite group.

References

Biagioni C., Moëlo Y., Favreau G., Bourgoin V. and Boulliard J.-C. (2015) Crystal structure of Pb-rich chabournéite from Jas Roux, France. *Acta Crystallographica*, **B71**, 81–88.

Ciobanu C.L., Brugger J., Cook N.J., Mills S.J., Elliott P., Damian G. and Damian F. (2014) Gražianite, $MnBi_2S_4$, a new mineral from the Băiţa Bihor skarn, Romania. *American Mineralogist*, **99**, 1163–1170.

Fershtater G.B. (2013) *Paleozoic Intrusive Magmatism of the Middle and Southern Urals*. Publishing house of RIO UB RAS, Ekaterinburg, Russia, 368 pp. [in Russian].

Kasatkin A.V., Nestola F., Agakhanov A.A., Škoda R., Karpenko V.Y., Tsyganko M.V. and Plášil J. (2018*a*) Vorontsovite, $(Hg_5Cu)_{\Sigma6}TlAs_4S_{12}$, and Ferrovorontsovite, $(Fe_5Cu)_{\Sigma6}TlAs_4S_{12}$: The Tl- and Tl-Fe-Analogues of Galkhaite from the Vorontsovskoe Gold Deposit, Northern Urals, Russia. *Minerals*, **8**, 185.

Kasatkin A.V., Makovicky E., Plášil J., Škoda R., Agakhanov A.A., Karpenko V.Y. and Nestola F. (2018*b*) Tsygankoite, $Mn_8Tl_8Hg_2(Sb_{21}Pb_2Tl)_{\Sigma24}S_{48}$, a New Sulfosalt from the Vorontsovskoe Gold Deposit, Northern Urals, Russia. *Minerals*, **8**, 218.

Kasatkin A.V., Makovicky E., Plášil J., Škoda R., Chukanov N.V., Stepanov S.Y., Agakhanov A.A. and Nestola F. (2019) Gladkovskyite, $MnTlAs_3S_6$, a new thallium sulfosalt from the Vorontsovskoe gold deposit, Northern Urals, Russia. *Journal of Geosciences*, **64**, 207–218.

Kasatkin A.V., Plášil J., Makovicky E., Škoda R., Agakhanov A.A., Stepanov S.Y. (2020) Luboržákite, IMA 2019-125; in: CNMNC Newsletter 54. *Mineralogical Magazine*, **84**, 359–365.

Kraus W. and Nolze G. (1996) POWDER CELL – a program for the representation and manipulation of crystal structures and calculation of the resulting X-ray powder patterns. *Journal of Applied Crystallography*, **29**, 301–303.

Makovicky E. (2006) Crystal structures of sulfides and other chalcogenides. Pp. 7–125 in: *Sulfide Mineralogy and Geochemistry* (D.J. Vaughan, editor). Reviews in Minralogy and Geochemistry, **61**. Mineralogical Society of America and the Geochemical Society, Chantilly, Virginia, USA.

Makovicky E. (2019) Algorithms for calculations of homologue order N in the homologous series of sulfosalts. *European Journal of Mineralogy*, **31**, 83–97.

Makovicky E., Mumme W.G. and Watts J.A. (1977) The crystal structure of synthetic pavonite, $AgBi_3S_5$, and the definition of the pavonite homologous series. *The Canadian Mineralogist*, **15**, 339–348.

Merlet C. (1994) An accurate computer correction program for quantitative electron probe microanalysis. *Microchimica Acta*, **114/115**, 363–376.

Minina O.V. (1994) The Auerbakh Complex ore-magmatic system of the Middle Ural. *Native Geology*, **7**, 17–23 [in Russian].

Mumme W. G. and Žák L. (1985) Paděraite, $Cu_{5.59}Ag_{1.3}Pb_{1.6}Bi_{11.2}S_{22}$, a new mineral of the cuprobismutite-hodrušite group. *Neues Jahrbuch für Mineralogie, Mitteilunghen*, **12**, 557–567.

Murzin V.V., Bushmakin A.F., Sustavov S.G. and Shcherbachov D.K. (1996) Clerite $MnSb_2S_4$ – a new mineral from Vorontsovskoye gold deposit in the Urals. *Zapiski Vserossijskogo Mineralogicheskogo Obshchestva*, **125**, 3, 95–101 [in Russian].

Murzin V.V., Naumov E.A., Azovskova O.B., Varlamov D.A., Rovnushkin M.Yu. and Pirajno F. (2017) The Vorontsovskoe Au-Hg-As ore deposit (Northern Urals, Russia): Geological setting, ore mineralogy, geochemistry, geochronology and genetic model. *Ore Geology Reviews*, **85**, 271–298.

Petříček V., Dušek M. and Palatinus L. (2014) Crystallographic computing system Jana2006: general features. *Zeitschrift für Kristallographie*, **229**, 345–352.

Pfitzner A. and Kurowski D. (2000) A new modification of $MnSb_2S_4$ crystallizing in the $HgBi_2S_4$ structure type. *Zeitschrift für Kristallographie*, **215**, 373–376.

Rigaku (2019) *CrysAlis CCD and CrysAlis RED*. Rigaku-Oxford Diffraction Ltd, Yarnton, Oxfordshire, UK.

Sheldrick G.M. (2015) SHELXT – integrated space-group and crystal-structure determination. *Acta Crystallographica*, **A71**, 3–8.

Stepanov S.Yu., Sharpenok L.N. and Antonov A.V. (2017) Fluid-Exposive breccias of the Vorontsovskoe Gold Deposit (The North Urals). *Zapiski RMO*, **1**, 29–43 [in Russian].

Vikentyev I.V., Tyukova E.E., Murzin V.V., Vikent'eva O.V. and Pavlov L.G. (2016) *Vorontsovsk Gold Deposit. Geology, Gold Modes, Genesis*. Fort Dialog-Iset, Ekaterinburg, Russia, 204 p. [in Russian].

Žák L. (1972) A contribution to the crystal chemistry of melanophlogite. *American Mineralogist*, **37**, 779–796.

Žák L. and Povondra P. (1981) Kutnohorite from the Chvaletice pyrite and manganese deposit, east Bohemia. *Tschermaks Mineralogische und Petrographische Mitteilungen*, **28**, 55–63.

Žák L., Syneček V. and Hybler J. (1974) Krupkaite, $CuPbBi_3S_6$, a new mineral of the bismuthinite-aikinite group. *Neues Jahrbuch für Mineralogie, Mitteilunghen*, **12**, 533–541.

Žák L., Frýda J., Mumme W. G. and Paar W. H. (1994) Makovickyite, $Ag_{1.5}Bi_{5.5}S_9$, from Baite Bihorului, Romania: The [4]P natural mineral member of the pavonite series. *Neus Jahrbuch für Mineralogie, Abhandlungen*, **168**, 147–169.